

**Alternative explanation for groundwater temperature variations near Yucca Mountain,  
Nevada**

Scott Painter, James Winterle, Amit Armstrong\*

Center for Nuclear Waste Regulatory Analyses

Southwest Research Institute

6220 Culebra Road, San Antonio, TX 78238

Phone: (210) 522-5182 Fax: (210) 522-5155

E-mail: [spainter@swri.org](mailto:spainter@swri.org)

\*Current Address: Compu Simulations, P.O. Box 312, Vancouver, WA 98666-0312

**Abstract.** Groundwater temperatures in the fractured volcanic aquifer near Yucca Mountain, Nevada have previously been shown to have significant spatial variability with regions of elevated temperatures coinciding roughly with near-vertical north-south trending faults. Previous investigators have suggested upwelling along faults from an underlying aquifer as a likely explanation for this groundwater temperature pattern. Using a coupled flow and heat transport model, we show that the thermal high coinciding with the Paintbrush fault zone can be explained without significant upwelling from the underlying aquifer. Instead, the thermal anomaly is consistent with thermal conduction enhanced slightly by buoyancy-driven vertical groundwater movement within the volcanic aquifer sequence. If more than  $\sim 700 \text{ m}^3/\text{day}$  of water enters the volcanic aquifer from below, then the calculated temperatures at the water table are significantly greater than the measured temperatures. These results have some important implications for

understanding the groundwater flow system at Yucca Mountain and also underscore the value of using temperature data to constrain groundwater flow models.

## Introduction

It is widely recognized that groundwater temperature data are valuable for constraining conceptual models of groundwater flow or for estimating hydrologic parameters. A variety of approaches are available, ranging from non-quantitative interpretations to purely numerical finite element or finite difference solutions. A popular approach is to use analytical or semi-analytical solutions applicable to simplified systems to relate observed temperature profiles to unknown recharge rates. For example, analytical solutions are sometimes used in combination with observed temperature profiles to estimate vertical flow in one-dimensional systems. Although these analytical approaches have undeniable utility for some types of flow systems, detailed system geometry and buoyancy effects are difficult to include and may be important for some flow systems. In this paper, we consider an example of such a system and show how simplified analyses can result in misleading interpretation.

We consider a fractured tuff aquifer near Yucca Mountain, Nevada, and use three-dimensional coupled groundwater flow and heat transport simulations to demonstrate that observed elevated groundwater temperature aligned with a local fault system can be explained without fault-zone recharge. Specifically, we show that the regions of elevated groundwater temperature, which had previously been attributed to fault zone recharge from below, can be mostly explained by the effect of the fault offset on the topography of the aquifer confining layers. The relevant processes, thermal conduction and buoyancy driven vertical flow, would be difficult to model without using three-dimensional numerical simulators that explicitly account for density dependent flow.

Early work on the use of groundwater temperature data included a one-dimensional analytical solution by Bredehoeft and Papadopoulos (1965) for steady-state heat and incompressible fluid flow. This type of solution is well suited for use in semi-confining formations where flow is predominantly vertical (Lu and Ge, 1996). For example, vertical leakage in semi-confining layers can be estimated where thermal properties and vertical temperature profiles are known (e.g., Sorey, 1971). Hydrologic properties of aquitards can be inferred from such vertical leakage estimates when no other hydrologic data are available (e.g., Mansure and Reiter, 1979). Estimates of vertical flux from this one-dimensional approach are sensitive to small temperature variations, and hence may be biased by vertical flows within the well bore (e.g., Mansure and Reiter, 1979) or in the disturbed zone around the well bore. Also, because a bore-hole temperature profile represents a relatively small zone surrounding a well, profiles from several bore holes are needed to obtain reasonable confidence in vertical flux estimates for heterogenous formations.

When temperature data are available from numerous well bores, two-dimensional methods are available to identify areas of vertical aquifer recharge. For example, Bodvarsson et al. (1982) developed a transient two-dimensional semi-analytical solution to estimate fault-zone recharge from horizontal temperature variability. The applicability of this approach is limited to relatively thin, horizontal aquifers because vertical temperature and velocity variations within the aquifer are ignored. Such two-dimensional approaches are also limited by the assumptions of parallel horizontal layer boundaries, which ignores potential effects of surface and layer topography on thermal conductance. Neglect of regional groundwater flow also limits this approach to areas where temperature gradients resulting from vertical recharge are large enough that the effects of horizontal flow on the temperature distribution are minimal. Bodvarsson et al. (1982) used their model to estimate recharge at the Susanville Geothermal Project, California, where fault-zone recharge is

relatively hot, resulting in a horizontal temperature gradient of about 40 °C per km perpendicular to the fault.

Based on the conceptual approach of Bodvarsson et al. (1982), it may seem reasonable to infer areas of fault-zone recharge where elevated groundwater temperatures are observed along large-offset faults. Indeed, fault-zone recharge has been suggested as a cause for elevated temperatures zones in the region of Yucca Mountain, Nevada (Fridrich et al., 1994; Sass et al., 1988, 1995). We focus on one particular fault zone and explore this issue in a more quantitative way using three-dimensional finite-difference simulations.

### **Background of Study Area**

Yucca Mountain, located approximately 175 km northwest of Las Vegas, Nevada, is being evaluated as a potential geologic repository for disposal of high-level nuclear waste. The saturated zone beneath Yucca Mountain (Luckey et al., 1996) consists of alternating layers of volcanic tuff that form four hydrostratigraphic units: two aquifers and two confining units (Figure 1). The volcanic tuffs overlie a regional, predominantly carbonate aquifer of Paleozoic origin that is largely confined in the vicinity of Yucca Mountain by the overlying thick sequence of low-permeability tuffs ( $k \sim 10^{-18} \text{ m}^2$ ), hereafter referred to as the lower confining layer. These aquifer and confining layers are offset by several north-south trending normal faults (Day et al. 1998), with displacements on the order of a few hundred meters (Figures 1 and 2). A question important to the performance of a proposed nuclear waste repository is whether these faults provide pathways for flow between the local volcanic tuff aquifer system and the regional Paleozoic carbonate aquifer system.

Of interest in this study are temperature measurements near the water table in the volcanic tuffs beneath Yucca Mountain (Sass et al. 1988) that reveal elevated water temperatures aligned

with the north-south trending Solitario Canyon fault and the Paintbrush-Bow Ridge fault system, as shown in Figure 2. Fridrich et al. (1994) and Sass et al. (1988, 1995) suggest that these observations could indicate upward flow along faults to the shallow saturated zone from a deeper aquifer, possibly the Paleozoic carbonate aquifer. Others have suggested that the cooler temperatures between the Solitario Canyon and Paintbrush fault zones, shown in Figure 2, could indicate a fast pathway for southward flow of cooler water that derives from surface recharge to the north (Lehman and Brown 1995).

Estimation of recharge to the volcanic aquifer along fault zones has proved difficult, as little is known about hydrologic properties of local faults, and only one well in the study area, UE-25 p#1 (p#1), penetrates the regional carbonate aquifer. The two-dimensional approach of Bodvarson et al. (1982) for estimating fault zone recharge from horizontal temperature variability is not applicable because, as previously mentioned, that method is valid for thin aquifers, whereas the volcanic tuff aquifer is generally about 500 m thick within the study area.

One-dimensional analyses, based on the approach of Bredehoeft and Papadopoulos (1965), are useful to evaluate the potential for vertical leakage to the volcanic aquifer through the lower confining unit. Temperature profiles for p#1 and several other deep wells in the area (summarized by Sass et al., 1988) all show thick sections within the lower confining layer (typically > 200 m) with linear temperature-depth profiles. A linear temperature-depth profile indicates a zone with no vertical flow component (Bredehoeft and Papadopoulos, 1965). This leads to a conceptual model of an areally continuous confining layer that is interrupted only where offset by faults. Sass et al. (1995) point to an inversion zone in well p#1, where temperature begins to decrease with depth, as evidence for upward flow of warmer water within the Paintbrush fault zone. This temperature inversion zone is associated with a fault zone that was recorded in the well log below the base of the

lower confining unit (Craig and Robison, 1984). It is not conclusive whether this fault zone flow continues upward through confining layer to the volcanic tuff aquifer. Another fault zone intersected by well p#1, recorded higher up within the confining unit (Craig and Robison, 1984), reveals no inversion in the temperature-depth profile.

Another attempt to evaluate fault zone recharge near Yucca Mountain was made by Bredehoeft (1997). He used the phase shift between the  $M_2$  Earth-tide signal and the pressure response observed in p#1 to evaluate potential inter-aquifer flow along the Paintbrush fault. A strong Earth-tide response with little phase shift is generally taken to indicate good vertical aquifer confinement (e.g., Rojstaczer and Riley 1990), but no significant phase shift between the  $M_2$  Earth-tide signal and the pressure response in well p#1 was observed (Galloway and Rojstaczer 1988). Bredehoeft (1997) estimated that upward recharge to the volcanic aquifer along the Paintbrush fault zone could be as little as zero or as great as 1000 m<sup>3</sup>/d without a significant phase shift in the Earth-tide response.

Geochemical data does not help much to further constrain the range of fault-zone recharge, as the available evidence is ambiguous. The U.S. Department of Energy (2000a) shows that chloride data support a hypothesis of very little or no fault-zone recharge to the volcanic aquifer. Chloride concentrations in the carbonate aquifer are nearly four times as great as chloride concentrations recorded for the volcanic aquifer in several wells near Yucca Mountain. Despite this large difference in chloride concentrations, no pattern of increased chloride is observed across fault zones in the volcanic aquifer suggesting little or no recharge of water from the carbonate aquifer. Stetzenbach et al. (2001) reach entirely different conclusions based on a principal component analysis (PCA) of 27 trace elements in waters sampled from 36 well and spring locations in Southern Nevada. They show that water in the volcanic aquifer east of Yucca Mountain bears a

trace-element signature similar to that of carbonate aquifer waters, and propose recharge from the carbonate aquifer along fault zones as a principal source of volcanic aquifer water.

Thus, evidence to support vertical influx along faults from the carbonate aquifer to the volcanic aquifer is limited to non-quantitative inferences made from horizontal temperature variability, an analysis of Earth-tide response that suggests such recharge must be limited, and two conflicting geochemical analyses.

### **Groundwater Model**

The model region is outlined in Figure 2. We focus on the area south and east of the proposed repository that is centered around the vicinity of well p#1 and the region of elevated temperature at the water table that coincides with the north-south trending Paintbrush-Bow Ridge fault zone. The Solitario Canyon fault zone is not included because a steep hydraulic gradient across this fault indicates hydrogeologic complexity that is beyond the scope of the present study. Based on well water-level measurements, hydraulic gradients throughout the chosen model domain are small, generally less than  $10^{-3}$  (Luckey et al., 1996), and allow for more straightforward definition of hydrologic boundary conditions.

For our simulations, we used the METRA module of the MULTIFLO multiphase thermal-hydrological-chemical simulator (Painter et al. 2001). METRA solves the coupled flow and heat transport equations using an integrated finite-volume discretization and a fully implicit time stepping method. Water density and viscosity variation with pressure and temperature are included in METRA by interpolating standard thermodynamic tables. These variations are small and often neglected in groundwater modeling, but are important in the present applications because small differences in water density may, under some conditions, lead to buoyancy-driven vertical flow.

The computational grid extends vertically from the water table, as interpolated from several wells in the region, to the top of the carbonate aquifer. The present model is divided into four hydrostratigraphic layers representing upper and lower volcanic aquifers and upper and lower confining layers (Figures 2 and 3), as described by Luckey et al. (1996). The layer thickness, topography, and fault displacements represented in the model are based on an independent hydrogeologic framework model developed from bore-hole stratigraphic logs and surface-based geophysics (Sims et al., 1999). The base of the model coincides with the bottom of the lower volcanic confining layer. To incorporate the spatial variability in the thickness of each unit, the elevation of the base of the model, and the elevation of the water table, the model domain was discretized into a non-uniform but logically rectangular grid of 59 x 49 x 20 cells in the North-South, East-West, and vertical dimensions.

Specification of the temperature boundary condition at the base of the model requires some knowledge of the temperature in the Paleozoic aquifer. At present, however, only well p#1 penetrates the Paleozoic aquifer in the model region. A temperature log from well p#1 (Craig and Robison, 1984) shows that temperature in the carbonate aquifer is nearly constant (55 °C) with depth for about 200 m directly below the confining unit, and then decreases by only about 2 °C in the next 400 m. Relatively constant temperature over such a thick interval is consistent with a permeable, vertically well-mixed aquifer system. Given this observation and the lack of direct information on spatial variability in groundwater temperature in the Paleozoic aquifer, we use a constant-temperature (55 °C) boundary condition at the base of the model. Note also, that the base of the model is not at a constant depth; it follows the interpreted topography of the carbonate aquifer system (Figure 3).

Temperatures at the water table are better defined by direct measurement. Water table temperatures were specified as 29, 30, and 34 °C for the east, north, and west sides, respectively. Water table temperature on the south side was assumed to vary linearly from 31 to 34 °C moving east to west. Temperatures were assumed to vary linearly with depth along the four vertical faces. Heat transport by conduction only was assumed for the top boundary. Specifically, heat conduction from the water table to the land surface was included in the model and temperature in the interior of the top face was allowed to vary in response. The temperature at the land surface was specified at 20 °C. In this manner, we account for the variable thickness of the unsaturated zone, which was calculated using a digital elevation map and subtracting the interpolated water table elevation.

Because surface recharge rates in this arid region are negligible relative to lateral flux, the top boundary was specified as a no-flow confining surface coincident with the interpolated water table elevation, which slopes to the southeast. In a perfectly calibrated version of such a model for a water-table aquifer, the pressure at the aquifer top should be zero. This pressure condition was used to calibrate the permeability of the hydrostratigraphic units region as discussed in the following section. A hydrostatic pressure boundary condition was prescribed for the vertical faces of the model with appropriate density corrections to account for the variable temperature. The base of the model was specified as a no-flow boundary for the initial calibration. After the initial calibration, however, an upward volumetric flow that varied between 0 and 1000 m<sup>3</sup>/day at the base of the model was specified at grid cells along a 10-km section of the Paintbrush fault zone. The purpose of varying the upward flux along the Paintbrush fault was to evaluate the effect of fault-zone flow on the observed temperature near the water table in well p#1.

## Initial Model Calibration

Prior to evaluating the effects of fault-zone recharge on temperature, initial calibration of the model was attained through selection of permeability values for the four hydrostratigraphic units to obtain a reasonable match to pressure heads at 12 observation points. A permeability value of  $2 \times 10^{-13} \text{ m}^2$  was used for the two aquifer units,  $2 \times 10^{-16} \text{ m}^2$  was used for the upper confining unit, and  $10^{-18} \text{ m}^2$  was used for the lower confining unit. These values are roughly consistent with a previous calibrated regional scale isothermal model (U.S. Dept of Energy, 2000b). To achieve an acceptable level of calibration, it was also necessary to decrease permeability for all layers by a factor of 10 in zone of  $10 \times 10 \times 20$  computational cells in the northwest corner of the model. Decreased permeability in this area is consistent with hydraulic conductivity estimates from aquifer pumping tests (see e.g., Luckey et al., 1996). Using these permeability values as a reference case, the maximum residual error, expressed in terms of pressure head, is 6.0 meters, and the root-mean-square (RMS) residual error for the 12 equally weighted observation points is 3.0 meters. Overall, the residual pressure heads are relatively small compared with the variations in water levels through the model region (~40 meters) and demonstrate that the hydraulic conductivities, boundary conditions, and water table elevations form a nearly self-consistent set.

Several sensitivity runs were performed to check the calibration with alternative permeability scenarios. Without the zone of decreased permeability in the northwest corner, for example, the maximum residual error is doubled. We also varied vertical and horizontal permeability along the Paintbrush fault Zone: we evaluated scenarios of increased vertical and horizontal permeability in the north-south direction by a factor of ten, decreased east-west permeability by a factor of ten, and various combinations of the two. This was done to evaluate conceptual models in which faults act as conduits to flow along the fault axis and act as barriers to

flow across the fault plane. We also evaluated global anisotropy with a north-south permeability tenfold greater than east-west permeability. None of these scenarios significantly improved the overall calibration of residual pressure heads, and several combinations resulted in worse calibration, suggesting that alteration of hydrologic properties in Paintbrush fault zone is not necessary to explain groundwater flow in the modeled region. Further, the calculated temperature distributions from these scenario analyses were similar to those obtained in the reference case.

## **Results**

Calculated temperature at the water table is shown as a contour plot in Figure 4 for the reference case with no upwelling from the carbonate aquifer. The region of enhanced groundwater temperature above the Paintbrush fault is accurately reproduced with zero upwelling from the underlying carbonate aquifer. The RMS temperature difference between the calculated temperature and temperature measured in the 12 calibration wells is less than 2 °C and residual errors are roughly symmetric around zero. In the northwest corner of the model region, however, calculated temperatures are generally lower than the observed values shown in Figure 2. The residual error in this region can be attributed to the assumed constant temperature of 55 °C specified for the entire bottom boundary. Indeed, temperatures in two deep wells in this area exceed 60 °C in the deeper parts of the lower confining layer.

The thermal high near the Paintbrush fault is caused in the model primarily, but not entirely, by the topographies of the volcanic and Paleozoic aquifers. The Paintbrush fault corresponds to a structural high in the underlying carbonate aquifer and it is expected that temperatures at the water table would be higher there since the thermal insulation effects of the volcanic tuff layers are reduced. To test this, we also constructed a heat-conduction only model using the same geometry.

As shown in Figure 5, this model does show a region of enhanced temperature along the Paintbrush fault, which suggests a dominant effect controlling the groundwater temperature is simply the geometry of the aquifer and aquitard layers combined with our assumption of a near-constant temperature in the underlying Paleozoic aquifer. However, the temperatures across the conduction-only model are systematically lower than the measured values compared to the reference case with groundwater flow. This result suggests that buoyancy-driven flow may also play a minor role. To explore this possibility further, we plot in Figure 6 values of vertical velocity at a model layer 15 (of 20) measured from the bottom and in cross section. Warm colors represent upward moving fluid and cool colors represent downward moving fluid. There are significant upward velocities on the upslope sides of the fault and downward velocities on the downslope sides consistent with free thermal convection. Although the groundwater velocity fields have upward- and downward-moving zones characteristic of the idealized convection cells familiar from theoretical studies of perfectly horizontal layers, the flow patterns are likely to be more complex than this because of the three-dimensional nature of the system.

Given the relatively low permeabilities and the modest thermal gradients in this system, the formation of free thermal convection currents may be surprising. Indeed, the Rayleigh number for the volcanic aquifer is orders of magnitude smaller than the Rayleigh-Lapwood criterion for the onset of convection in a horizontal porous medium heated from below (see, e.g., Domenico and Schwartz 1990). However, the Rayleigh-Lapwood and related criteria are specific to the situation where isotherms and geopotentials are aligned. There is no threshold for free convection when the temperature gradient and body forces are not aligned. In our model, buoyancy-driven upward flow occurs near the Paintbrush fault zone because of the steep slope in the constant-temperature base of the model in that area.

Figure 7 shows the calculated temperature at the location of well p#1 well as a function of the total incoming volumetric flow rate from the carbonate to the volcanic aquifer. For these calculations, we specified an upward flow into the model domain for those cells on the lower boundary that also intersect the Paintbrush fault. The observed temperature at well p#1 and the temperature as calculated by the conduction only model are also shown. The calculated and observed temperatures coincide when the incoming flow rate is about 400 m<sup>3</sup>/day. However, there is some uncertainty in the calculated (and probably also the measured) temperatures coming from uncertainty in the input parameters, and the situation of no recharge from below probably cannot be dismissed. The situation of 1000 m<sup>3</sup>/day fault-zone recharge – the suggested upper bound from Bredehoeft (1997) – results in a calculated temperature that is 6 °C larger than the measured water-table temperature in well p#1.

### **Discussion and Conclusions**

Our numerical model suggests that the regions of enhanced temperature along the Paintbrush fault zone can be explained without invoking significant vertical recharge from the underlying Paleozoic aquifer. The region of elevated temperature can be explained instead by heat conduction enhanced slightly by buoyancy-driven vertical flow within the volcanic aquifer. The effect is largely due to the geometry of the system; the region of elevated temperature coincides with a structural high in the Paleozoic aquifer where the insulating effect of the volcanic tuff sequence is reduced.

The main motivation for this work is to better understand the possible hydraulic communication between the volcanic and Paleozoic aquifers in the Yucca Mountain region with the eventual goal of better understanding groundwater flow and travel times from the proposed

repository to potential pumping locations. Based on the modeling, the best estimate of recharge from the Paleozoic aquifer along the Paintbrush fault zone is 400 m<sup>3</sup>/day. However, there is uncertainty in the calculated temperatures related to the uncertainties in boundary conditions, etc. For example, if we assume an uncertainty of  $\pm 1.5$  °C for the calculated temperatures in Figure 7, then the recharge rate is estimated to fall in the range 0–700 m<sup>3</sup>/day for the entire 10-km length of the Paintbrush fault zone in the modeled region. This range of recharge rates is also consistent with the estimate of 0–1000 m<sup>3</sup>/day by Bredehoeft (1997) based on the earth-tide signal in the carbonate aquifer at well p#1. This range of fault-zone recharge is small compared to the lateral fluxes across the model region.

Because of the limited spatial extent of the model region, these results cannot be used to make direct conclusions about other fault zones in the Yucca Mountain area. However, the results do suggest that inferences about groundwater fluxes that are based solely on qualitative interpretation of temperature data should be viewed with caution until they are backed up with more quantitative analyses that consider buoyancy effects and the detailed geometry of the system.

This latter point also applies in a more general context. Clearly temperature data can provide valuable constraints on groundwater flow, but inferences based solely on qualitative interpretations of thermal anomalies may be misleading. Several computer codes are available to solve coupled heat transport and water movement while taking into account temperature dependencies in water density and viscosity. These coupled heat and flow models may be combined with borehole temperature measurements to reduce uncertainties in groundwater flow models.

## **Acknowledgments**

This paper documents work performed by the Center for Nuclear Waste Regulatory Analyses under contract No. NRC-02-97-009. The work is an independent product and does not necessarily reflect the regulatory position of the NRC. The authors are grateful to Drs. B. Sagar and C. Manepally for their careful review of the manuscript.

## References

- Bodvarsson, G.S., S.M. Benson, and P.A. Witherspoon. 1982. Theory or the development of geothermal systems charged by vertical faults, *Journal of Geophysical Research* 87, no. B11: 9317–9328.
- Bredehoeft, J.D., and I.S. Papadopoulos. 1965. Rates of vertical groundwater movement estimates from the Earth's thermal profile, *Water Resources Research* 1, no. 2: 325–328.
- Bredehoeft, J.D. 1997. Fault permeability near Yucca Mountain. *Water Resources Research* 33, no. 11: 2459–2463.
- Craig, R.W., and J.H. Robison. 1984. *Geohydrology of Rocks Penetrated by Test Well UE-25p#1*. Water Resources Investigations Report 84–4248. Denver, CO: U.S. Geological Survey.
- Day, W.C., R.P. Dickerson, C.J. Potter, D.S. Sweetkind, C.A. San Juan, R.M. Drake II, and C.J. Fridrich. 1998. *Bedrock Geologic Map of the Yucca Mountain Area, Nye County, Nevada*. U.S. Geological Survey Geologic Investigations Series Map I–2627. Denver, Colorado.
- Domenico, P.A., and F.W. Schwartz. 1990. *Physical and Chemical Hydrogeology*, New York: John Wiley and Sons.

- Fridrich, C.J., W.W. Dudley Jr., and J.S. Stuckless. 1994. Hydrogeologic analysis of the saturated-zone ground-water system, under Yucca Mountain, Nevada. *Journal of Hydrology* 154: 133–168.
- Galloway, D., and S. Rojstaczer. 1998. Analysis of the frequency response of water levels in well to earth tides and atmospheric loading. In *Proceedings Fourth Canadian/American Conference on Hydrogeology*, ed. Hitchon et al. Dublin, Ohio: National Groundwater Association.
- Lehman, L.L. and T.P. Brown. 1995. An alternative conceptual model for the saturated zone at Yucca Mountain. Proceedings, *Waste Management '95*, Tucson, Arizona: Univ. of Arizona.
- Lu, N. and S. Ge. 1996. Effect of horizontal heat and fluid flow on the vertical temperature distribution in a semiconfining layer. *Water Resources Research* 32, no. 5: 1449–1453.
- Luckey, R.R., P. Tucci, C.C. Faunt, E.M. Ervin, W.C. Steinkampf, F.A. D'Agnese, and G.L. Patterson. 1996. *Status of understanding of the saturated-zone ground-water flow system at Yucca Mountain, Nevada, as of 1995*. U.S. Geological Survey Water-Resources Investigations Report 96–4077. Denver, Colorado.
- Mansure, A.J. and M. Reiter. 1979. A vertical groundwater movement correction for heat flow, *Journal of Geophysical Research* 84, no. B7: 3490–3496.

Painter, S., P.C. Lichtner, and M. Seth. 2001. MULTIFLO Version 1.5: Two-phase non-isothermal coupled thermal hydrological chemical flow simulator. Center for Nuclear Waste Regulatory Analyses. San Antonio, Texas.

Rojscaczer, S. and F.S. Riley. 1990. Response of the water level in a well to earth tides and atmospheric loading under unconfined conditions. *Water Resources Research* 26, no. 8: 1803–1817.

Sass, J.H., W.W. Dudley Jr., and A.H. Lachenbruch. 1995. Regional Thermal Setting. Chapter 8 of *Major Results of Geophysical Investigations at Yucca Mountain and Vicinity, Southern Nevada*, ed. H.W. Oliver, D.A. Ponce, and W.C. Hunter. U.S. Geological Survey Open-File Report 95–74. Menlo Park, California.

Sass, J.H., Lachenbruch, A.H., Dudley, W.W., Jr., Priest, S.S., and Munroe, R.J. 1988. *Temperature, Thermal Conductivity, and Heat Flow Near Yucca Mountain, Nevada: Some Tectonic and Hydrologic Implications*. U.S. Geological Survey Open-File Report 87–649. Denver, Colorado.

Sims, D.W., J.A. Stamatakos, D.A. Ferrill, H.L. McKague, D.A. Farrell, A. Armstrong. *Three Dimensional Structural Model of the Amargosa Desert, Version 1.0*: Report to Accompany Model Transfer to the Nuclear Regulatory Commission. CNWRA Letter Report. San Antonio, TX: Center for Nuclear Waste Regulatory Analyses. 1999.

Sorey, M.L. 1971. Measurement of vertical groundwater velocity from temperature profiles in wells. *Water Resources Research* 7, no. 4: 963–970.

Stetzenbach, K.J., V.F. Hodge, C. Guo, I.M. Farnham, and K.H. Johannesson. 2001. Geochemical and statistical evidence of deep carbonate groundwater within overlying volcanic rock aquifers/aquitards of southern Nevada, USA. *Journal of Hydrology* 243: 254–271.

U.S. Dept. of Energy. 2000a. *Geochemical and Isotopic Constraints on Groundwater Flow Directions, Mixing, and Recharge at Yucca Mountain, Nevada*. Civilian Radioactive Waste Management, Management and Operating Contractor, Analysis/Model Report ANL-NBS-HS-000021, REV 00.

U.S. Dept. of Energy. 2000b. *Calibration of the Site-Scale Saturated Zone Flow Model*. Civilian Radioactive Waste Management, Management and Operating Contractor, Process Model Report MDL-NBS-HS-000011, REV 00.

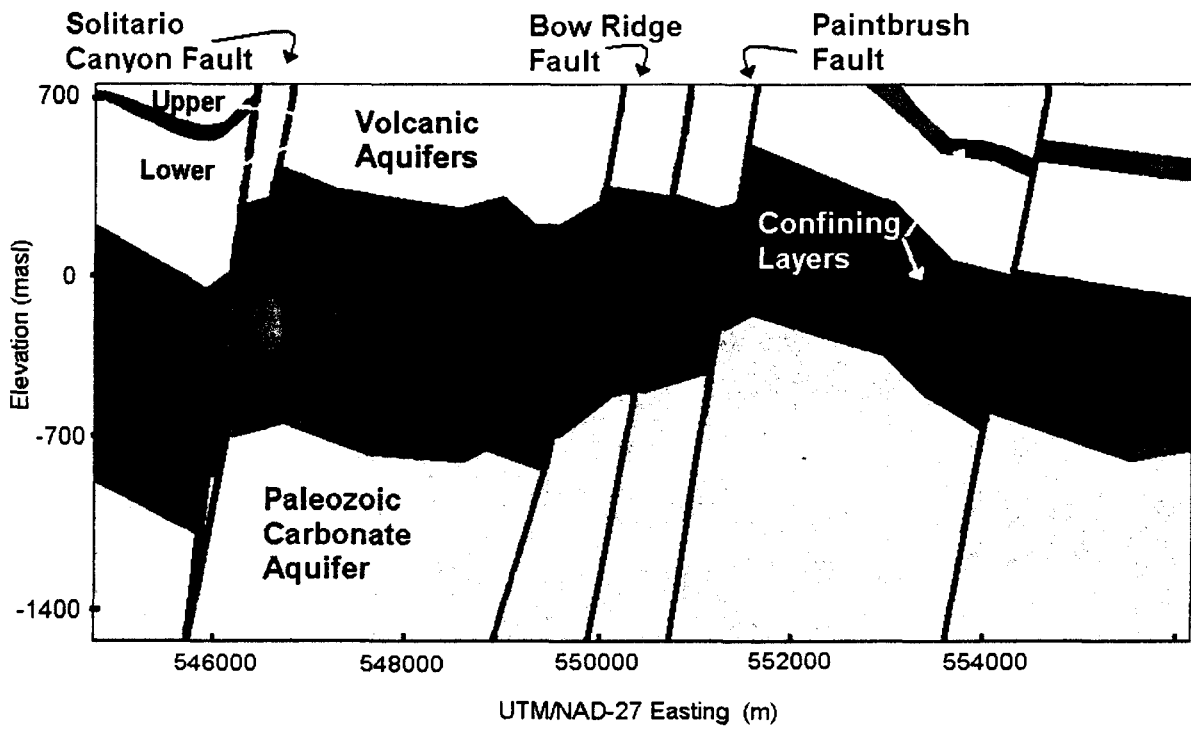


Figure 1. Cross section through study area along UTM/NAD-27 Northing 4074000. Non-isothermal groundwater flow in the region between the Paleozoic aquifer and the water table was modeled. Heat conduction across the unsaturated zone (not shown) was included in the model

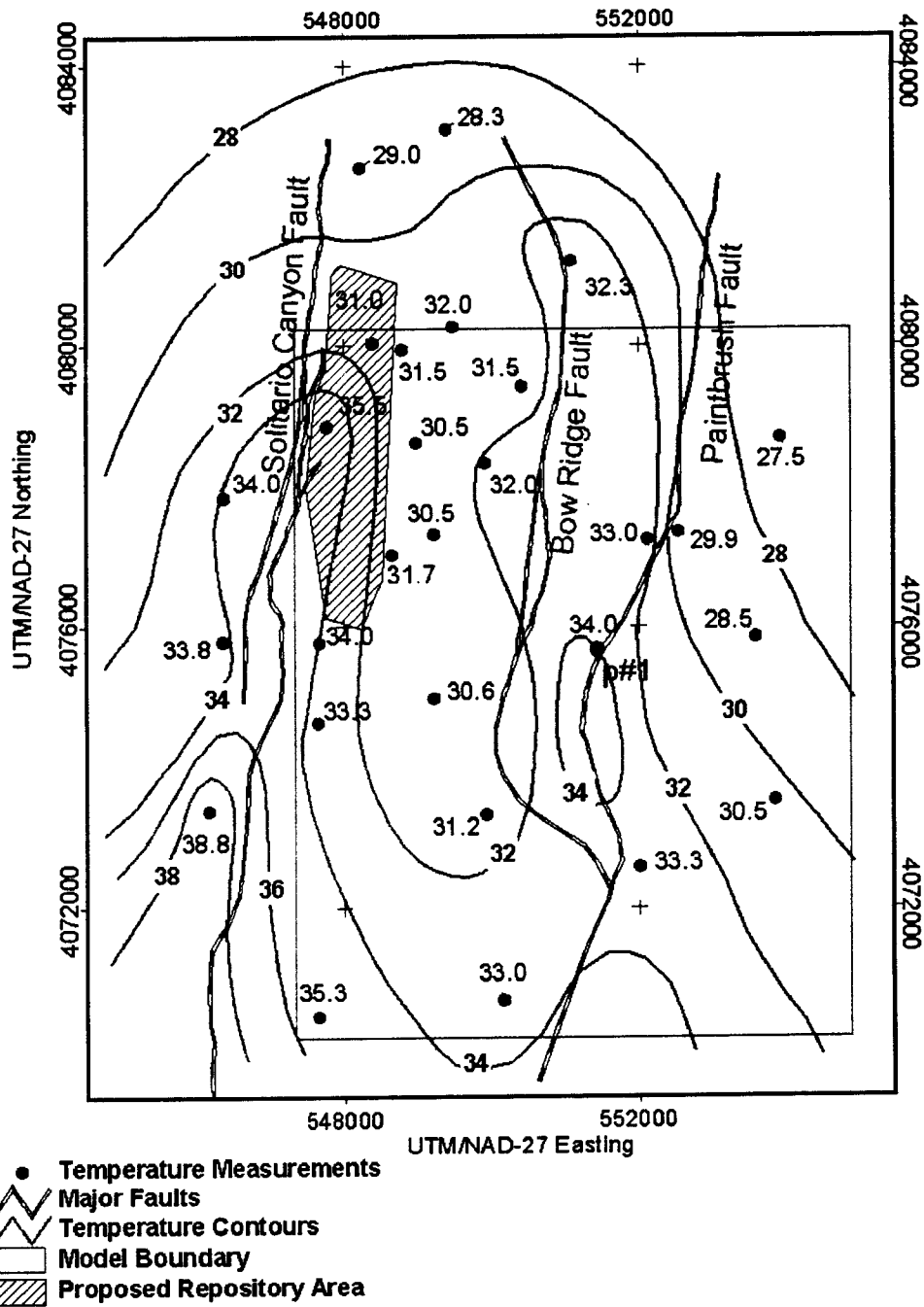


Figure 2. Map of study area showing surface traces of faults with offsets > 100 m (Day et al., 1998), groundwater temperatures near the water table (Sass et al., 1995), and an interpretation of groundwater temperature contour lines (modified from Sass et al., 1995). The model domain is also outlined.

12/14

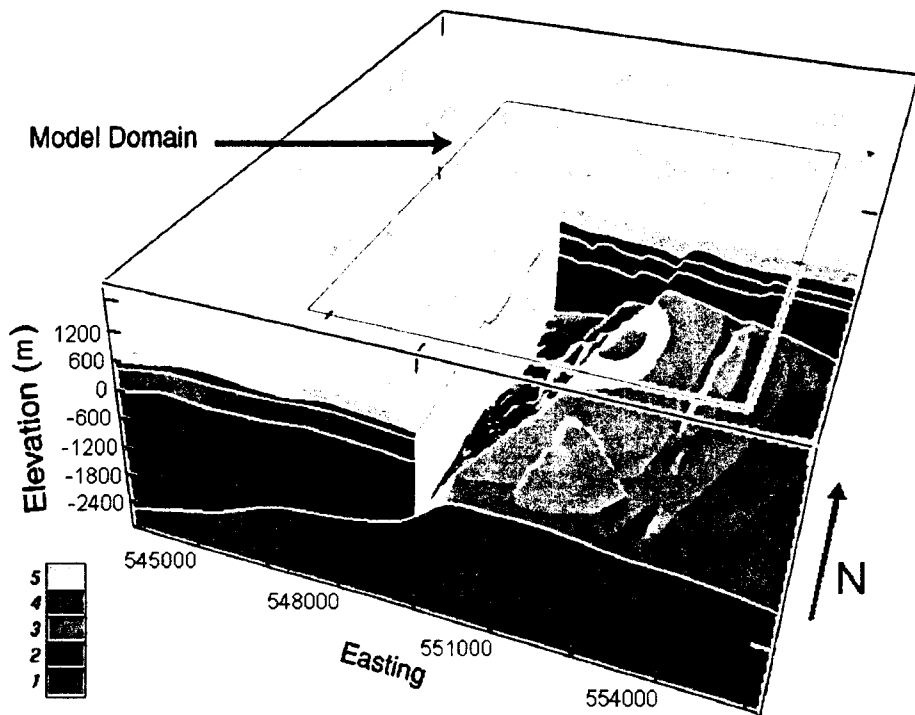


Figure 3. Three-dimensional perspective on the modeling domain showing hydrostratigraphic units: (1) regional carbonate aquifer (not modeled), (2) lower volcanic confining unit, (3) lower volcanic aquifer, (4) upper volcanic confining unit, and (5) upper volcanic aquifer. Color contours in cutaway indicate topographic relief of the carbonate-tuff boundary used as bottom model boundary.

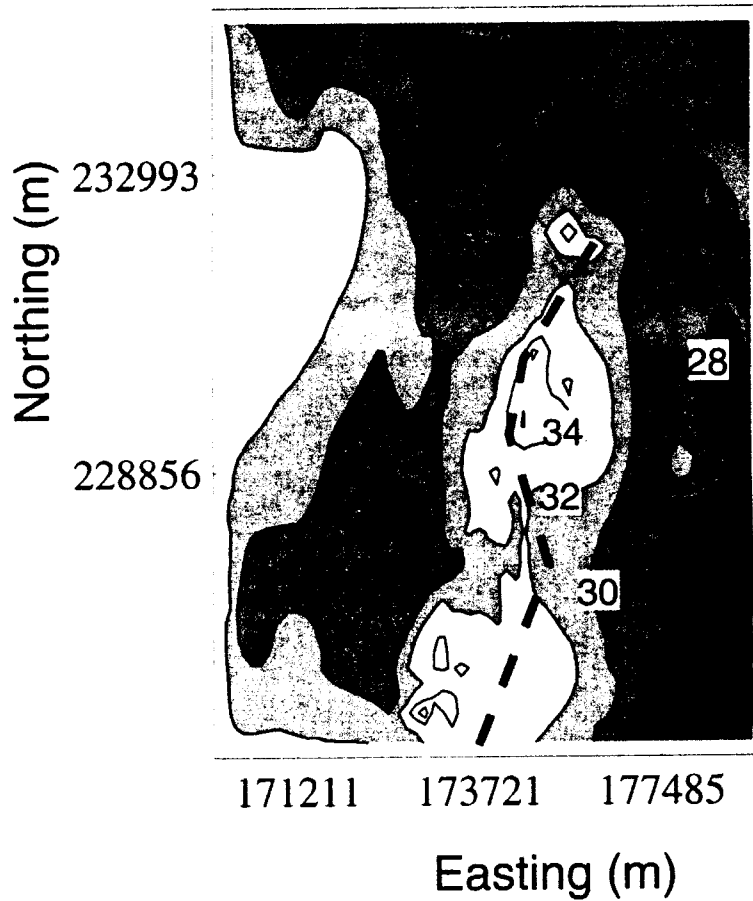


Figure 4. Contours of calculated temperature ( $^{\circ}\text{C}$ ) at the water table for the reference case with no fault-zone recharge. The region of elevated temperature corresponds with the Paintbrush fault zone. Note the similarity with the interpreted temperature contours in Figure 2.

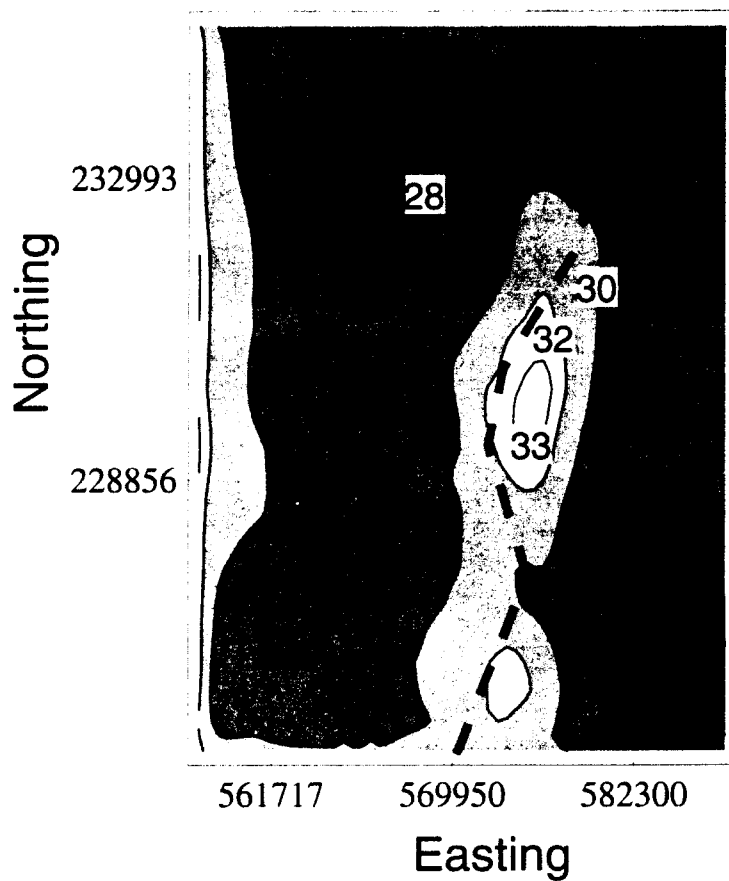


Figure 5. Contours of calculated temperature ( $^{\circ}\text{C}$ ) at the water table based on thermal conduction only.

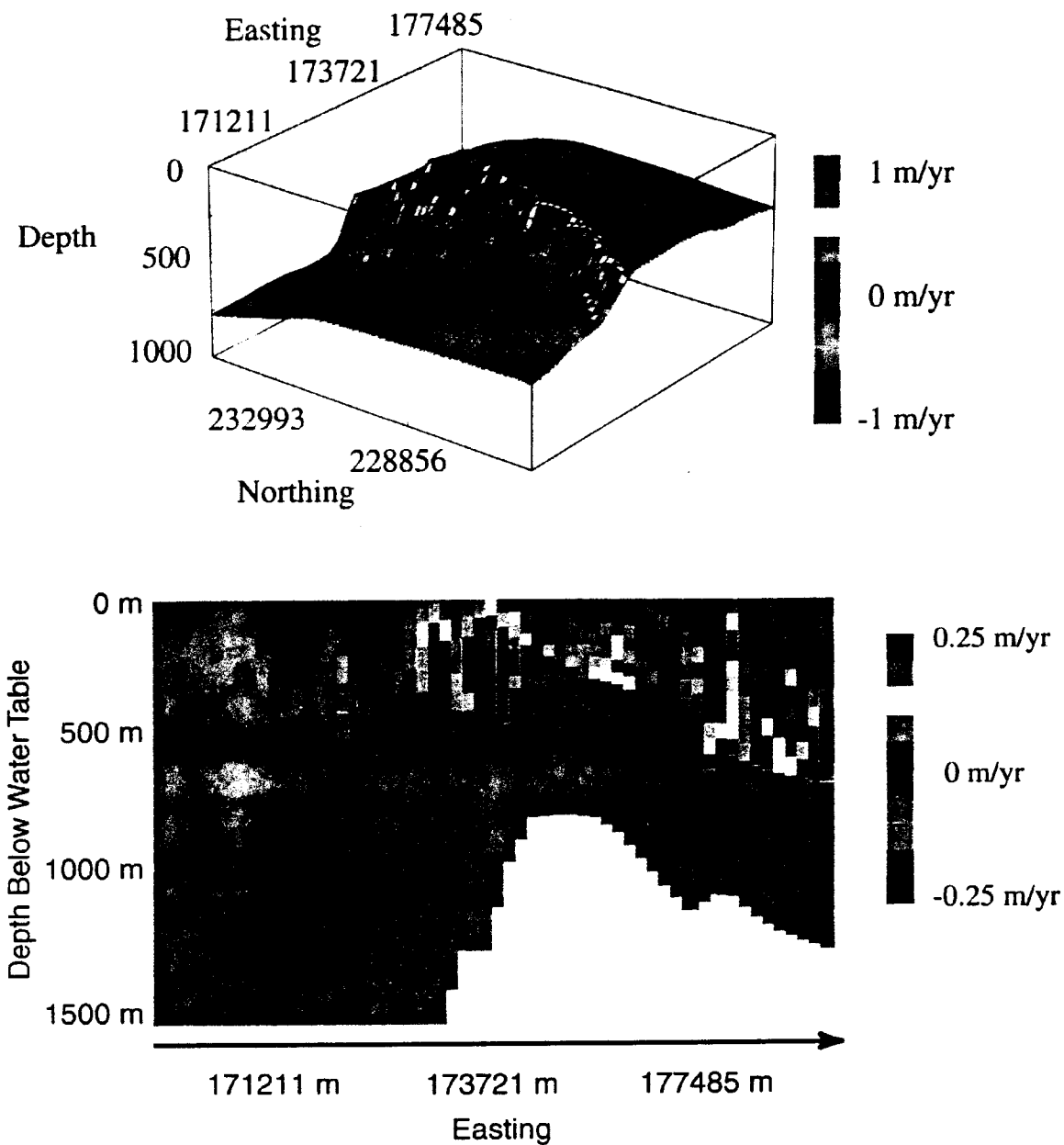


Figure 6. Vertical Darcy velocity at (a) the surface coinciding with computational layer 15 (of 20) measured from the bottom of the model, and (b) a horizontal cross section nearly equidistant between the south and north faces. Warm colors represent upward moving fluid. Water is moving upward on the upslope sides of the faults and downward on the downslope sides. The largest vertical Darcy velocity occurs in the aquifer units.

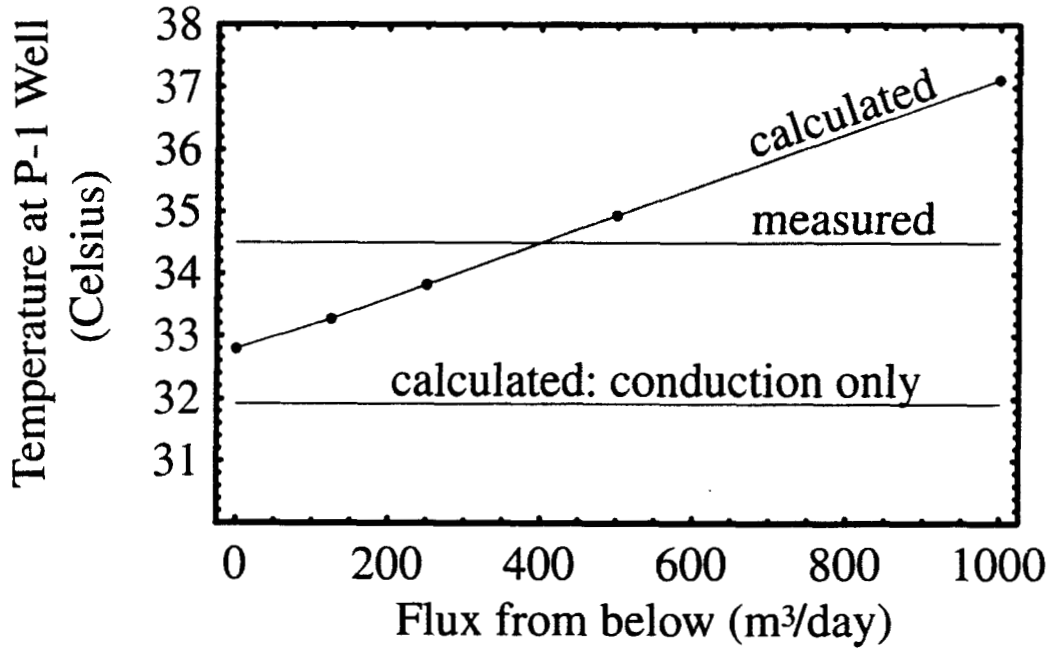


Figure 7. Calculated temperature at the water table at the location of the p#1 well as function of vertical flux through the Paintbrush fault zone. The measured temperature is shown for comparison purposes.